

## A SIMPLE MODEL OF THE BATCH ELECTROCHEMICAL REDUCTION OF NITRATE/NITRITE WASTE (U)

by

Hobbs, D.T.

Westinghouse Savannah River Company  
Savannah River Site  
Aiken, South Carolina 29808

Wingard, D.A.  
University of South Carolina

Weidner, J.W.  
University of South Carolina

Van Zee, J.W.  
University of South Carolina

A document prepared for PROCEEDING OF THE ELECTROCHEMICAL SOCIETY MEETING at San Francisco, CA, USA from 22 May - 27 May 1994.

DOE Contract No. DE-AC09-89SR18035

This paper was prepared in connection with work done under the above contract number with the U. S. Department of Energy. By acceptance of this paper, the publisher and/or recipient acknowledges the U. S. Government's right to retain a nonexclusive, royalty-free license in and to any copyright covering this paper, along with the right to reproduce and to authorize others to reproduce all or part of the copyrighted paper.

MASTER

DISTRIBUTION OF THIS DOCUMENT IS UNLIMITED

875

## DISCLAIMER

This report was prepared as an account of work sponsored by an agency of the United States Government. Neither the United States Government nor any agency thereof, nor any of their employees, makes any warranty, express or implied, or assumes any legal liability or responsibility for the accuracy, completeness, or usefulness of any information, apparatus, product, or process disclosed, or represents that its use would not infringe privately owned rights. Reference herein to any specific commercial product, process, or service by trade name, trademark, manufacturer, or otherwise does not necessarily constitute or imply its endorsement, recommendation, or favoring by the United States Government or any agency thereof. The views and opinions of authors expressed herein do not necessarily state or reflect those of the United States Government or any agency thereof.

This report has been reproduced directly from the best available copy.

Available to DOE and DOE contractors from the Office of Scientific and Technical Information, P. O. Box 62, Oak Ridge, TN 37831; prices available from (615) 576-8401.

Available to the public from the National Technical Information Service, U. S. Department of Commerce, 5285 Port Royal Rd., Springfield, VA 22161

## **DISCLAIMER**

**Portions of this document may be illegible in electronic image products. Images are produced from the best available original document.**

## **A Simple Model of the Batch Electrochemical Reduction of $\text{NO}_3^-/\text{NO}_2^-$ Waste**

Donald A. Wingard, John W. Weidner, John W. Van Zee  
Chemical Engineering Department  
University of South Carolina, Columbia, SC 29208  
and  
David T. Hobbs  
Westinghouse Savannah River Company  
Savannah River Laboratory, Aiken, SC 29808

### **Abstract**

A model of a divided parallel plate electrochemical cell operated in a batch mode for the destruction of  $\text{NO}_3^-/\text{NO}_2^-$  in alkaline waste streams is presented. The model uses boundary layer approximations at each electrode and at the separator to minimize computation time. Five competing electrochemical reactions are included at the cathode. The model uses either an explicit Runge-Kutta routine with empirically determined current efficiencies or an implicit stepping routine for each electrode if the current efficiencies are to be predicted. Time dependent changes of the concentration, temperature, and cell voltage are predicted for constant current operation. Model predictions are compared with experimental data.

### **Introduction**

The electrochemical treatment of liquid radioactive wastes has become a topic of scientific and environmental interest in recent years. In particular, methods of electrochemically reducing  $\text{NO}_3^-/\text{NO}_2^-$  wastes to NaOH holds promise in decreasing the waste volume and the possible reuse, after evaporation, as a pure stream of concentrated NaOH [1]. Preliminary experimental data has been collected [2] using a parallel plate electrolyzer with a divided cell configuration. Here, a simple model has been developed to predict concentration and temperature changes in this parallel plate cell using empirical correlations and assumptions generated from the experimental data.

The anolyte and catholyte are recirculated through the cell and into mixing reservoirs. Typically the residence time is short and conversions per pass are small in the reactor due to the goal of operating at a high limiting current. At the start of batch operation, the catholyte is a synthetic waste stream composed of 1.95 M  $\text{NaNO}_3$ , 0.60 M  $\text{NaNO}_2$ , and 1.33 M NaOH and the anolyte is approximately 5.0 M NaOH. In the model,

the well-mixed reservoirs of the anolyte and catholyte and the parallel plate cell are lumped together and treated as batch reactors with gas generation. Material balances are solved for these reservoirs using an explicit Runge-Kutta or an implicit stepping routine to integrate the equations. The model predicts the concentration, voltage and temperature changes during a batch operation. Energy balances are solved to predict temperature changes due to heat transfer and voltage losses within the electrochemical cell. The model considers five competing electrochemical reactions at the cathode and only the oxidation of  $\text{OH}^-$  at the anode. An alternative to the model presented here is a more rigorous single-pass model [3].

Figure 1 is a schematic diagram of the experimental apparatus in which storage tanks #1 and #2 correspond to the anolyte and catholyte reservoirs respectively. For batch operation, storage tanks #3 and #4 are not used and the solutions are returned to tanks #1 and #2 through valves throughout the run. In a typical experiment, anolyte and catholyte solutions are charged into the system. The pumps are then turned on and the rotameters adjusted to the desired flowrates. A constant current is then applied to the electrochemical cell. Anolyte and catholyte samples are collected during the course of the experiment from which concentration data is obtained for the major components. Reservoir temperatures are recorded for the duration of the experiment. The experiment is terminated when approximately 95% of the initial  $\text{NO}_3^-$  and  $\text{NO}_2^-$  is destroyed.

## Theory and Mathematical Model

### Model Equations

The voltage of the cell depends on the open circuit potential of the cell ( $V_o$ ), the resistances of the anolyte, catholyte, and separator ( $R_a$ ,  $R_c$ , and  $R_s$ ), the current density through the cell ( $i$ ), and the kinetic and concentration overpotentials at the anode and cathode ( $\eta_a$  and  $\eta_c$ ):

$$V = V_o + iAR_{cell} + |\eta_a| + |\eta_c| \quad (1)$$

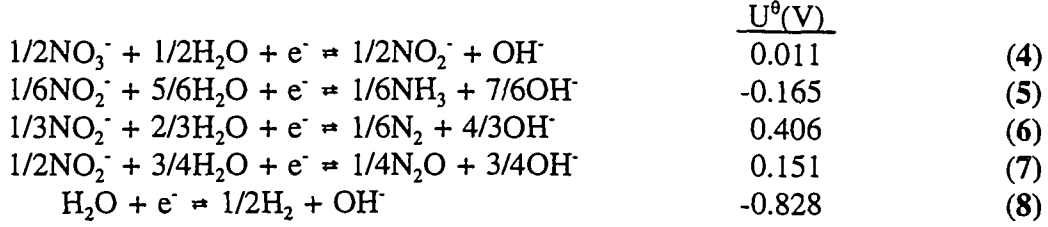
where,  $A$ , is the projected electrode area in the parallel plate cell. The open circuit potential of the cell is the difference between the thermodynamic potential of the anode ( $U_a$ ) and the mixed potential of the cathode ( $E_c$ ):

$$V_o = E_c - U_a \quad (2)$$

The anodic reaction is the oxidation of  $\text{OH}^-$  to form  $\text{O}_2$  and the thermodynamic voltage should deviate from an initial anode voltage as the activities of the anolyte and the temperature change:

$$U_a = U_a^\theta - \frac{RT}{4F} \ln \left( \frac{a_{H_2O}^2 P_{O_2}}{a_{OH^-}^4} \right) \quad (3)$$

The voltage of the cathode ( $E_c$ ) is a mixed potential corresponding to the combined effects of thermodynamics and kinetics of  $NO_3^-/NO_2^-$  reduction and the water reduction reaction. These reactions can be written:



The resistance in the cell depends on the conductivity of the anolyte, catholyte, and separator ( $\kappa$ ). It is also directly dependent on the perpendicular distances ( $S_i$ ) through the electrolytes and separator between the parallel plates of the cell:

$$R_{cell} = \frac{1}{A} \left( \frac{S_a}{\kappa_a} + \frac{S_s N_M}{\kappa_s} + \frac{S_c}{\kappa_c} \right) \quad (9)$$

The constant, A, is the projected area of the electrodes and  $N_M$ , the MacMullin number [4], is a property of the separator which may be defined as the ratio of the porosity to the tortuosity. Experimental data are used to develop empirical correlations for the conductivity which is a function of concentrations and temperature.

The overpotentials at the anode or cathode may be determined by using the Butler-Volmer equation:

$$\frac{i_j}{i_{o_j,ref}} = \prod_k \left( \frac{C_k}{C_{k,ref}} \right)^{p_{kj}} \exp \left( \frac{\alpha_{aj} F}{RT} \eta_j \right) - \prod_k \left( \frac{C_k}{C_{k,ref}} \right)^{q_{kj}} \exp \left( \frac{-\alpha_{cj} F}{RT} \eta_j \right) \quad (10)$$

In which k is the ionic species and j is the corresponding reaction. The overpotential ( $\eta_j$ ), in equation 10, is the difference between the voltage of the electrode, the solution potential at the electrode surface, and the reference electrode potential. For a single reaction, the boundary layer assumption results in an expression for the ratio of the surface concentration,  $C_k$ , to the reference concentration,  $C_{k,ref}$ , in terms of the limiting current [5]:

$$\frac{C_k}{C_{k,ref}} = \left( 1 - \frac{i}{i_{Lk}} \right) \frac{C_{k,b}}{C_{k,ref}} \quad (11)$$

where the limiting current density for species k at the anode and cathode may be calculated:

$$i_{Lk} = \frac{Nu_k D_k F C_k n}{s_k L} \quad (12)$$

Newman [6] gives an expression for the average Nusselt number for flow between two planar electrodes:

$$Nu_k = 1.8488 \left( \frac{Re Sc_k d_e}{L} \right)^{1/3} + 0.4 \quad (13)$$

in which

$$Re = \frac{d_e v}{\nu} \quad (14)$$

and

$$Sc_k = \frac{\nu}{D_k} \quad (15)$$

For multiple reactions, the concentration ratio includes the sum of the partial current densities since the flux of species k at the surface depends on all of the j reactions:

$$\sum \frac{-s_j i_j}{n_j F} = N_k = k_{mk} (C_{kb} - C_k) \quad (16)$$

where  $k_{mk}$  is the mass transfer coefficient for species k,  $C_{kb}$  is the bulk concentration and  $C_k$  is the surface concentration of species k. The mass transfer coefficient can be calculated from the following equation:

$$k_{mk} = \frac{Nu_k D_k}{2S} \quad (17)$$

Thus the concentration ratio in the Butler-Volmer equation can be written:

$$\frac{C_k}{C_{k,ref}} = \left( 1 - \frac{\sum \frac{s_{ij}^i j}{n_j F}}{k_{mk} C_{kb}} \right) \frac{C_{kb}}{C_{k,ref}} \quad (18)$$

These concentration ratios are then included in the Butler-Volmer equation with the assumed fractional reaction orders shown in Table I. As discussed below the prediction of the partial current densities for multiple reactions using this boundary layer approximation results in a set of nonlinear ordinary equations which must be solved at each time step. These equations can be contrasted to the equations of the more rigorous model which requires solution of a set of nonlinear equations at each spatial position.

### Mass Balances

The change in the liquid phase molar concentration of species  $i$  is governed by a time dependent mole balance which may be written in a form:

$$\frac{d(VC_k)}{dt} = Q_{in} C_{k,in} - Q_{out} C_{k,out} - \sum_j \frac{s_{kj} i A \epsilon_j}{n_j F} + R_k \quad (19)$$

The first two terms on the right hand side of equation (19) correspond to the inlet and outlet molar flows which may be set equal to zero since the reservoirs of the electrochemical cell are considered to be batch reactors. The third term is the electrochemical production of species  $i$  and the fourth term is the homogeneous production rate which may be set equal to zero. The change in concentration of each species depends only on the volume change in the reactor and the partial current densities which can be written as the product of the total applied current and reaction efficiencies or as the partial current densities as determined from the solution of the Butler Volmer Equations:

$$\frac{d(VC_k)}{dt} = - \sum_j \frac{s_{kj} i A \epsilon_j}{n_j F} - \sum_j \frac{s_{kj} i_j A}{n_j F} \quad (20)$$

In equations 4-8 the liquid species of interest are  $\text{NO}_3^-$ ,  $\text{NO}_2^-$ , and  $\text{OH}^-$  and the off-gas species  $\text{N}_2$ ,  $\text{NH}_3$ ,  $\text{N}_2\text{O}$ ,  $\text{H}_2$ , and  $\text{O}_2$ . The stoichiometric coefficients ( $s_{ij}$ ) may be obtained by placing the electrochemical reactions in a generalized form (see Newman [6]). The efficiencies,  $\epsilon_j$ , would typically be determined from empirical expressions but this empiricism is not needed if the partial current densities are obtained by solving simultaneously the partial current density equations (10) and an equation which requires the sum of the partial current densities to equal the total applied current at an electrode. The dependent variables in this problem are the solution potential at the electrode surface



and the five partial current densities corresponding to equations 4-8. During this calculation, the bulk concentrations are held constant at the inlet concentrations at that instant in time.

### Energy Balance

The energy balance for the batch reactor system can be written to include the enthalpies of the gas streams leaving the reservoirs:

$$V\rho C_p \frac{dT}{dt} = -(|\eta_a| i + \sum_{j=1}^M |\eta_{c_j}| i_{c_j}) A - (iA)^2 R_{cell} \quad (21)$$

$$+ UA(T_{Air} - T) - QC_{pgas} T$$

The first term on the right hand side corresponds to the summation of the energy losses at the anode and cathode due to kinetics and mass transfer. The second term corresponds to internal resistance losses due to the anolyte, catholyte, and separator. The third and fourth terms are the energy loss due to heat transfer to the atmosphere and the off gas leaving the reservoirs, respectively.

The variables  $C_p$  and  $\kappa_i$  are calculated using empirical expressions that are a function of concentration and temperature. Other physical parameters may be correlated to empirical equations as more experimental data becomes available.

### Results and Discussion

The simple model presented here differs from the differential [3] model in that it does not account for the effects of migration in the electrochemical cell. However, it does predict temperature which has a pronounced effect on reaction kinetics due to the dependency of the diffusion coefficients, reference potentials, limiting current densities, and electrical conductivities on temperature. The assumption of Tafel kinetics in the Butler-Volmer equation showed acceptable qualitative agreement with the rigorous model. The simple model converges rapidly with a computer run time of less than two minutes in most cases and may be adapted to spreadsheet software. Future use of the model includes the calculation of kinetic parameters from experimental data collected.

The physical and kinetic properties used in the model are shown in Table 1. Some values such as the exchange current densities and transfer coefficients are approximated due to the lack of experimental data. The initial concentrations of  $\text{NO}_3^-$ ,  $\text{NO}_2^-$ , and  $\text{OH}^-$  correspond to zero time in the simple numerical model.

Figures 3 and 4 show the current efficiencies of the cathodic reactions as a function of the charge passed through the electrochemical cell at current densities of  $0.35 \text{ A/cm}^2$  and  $0.45 \text{ A/cm}^2$  respectively. In the predictions the current efficiency for the reduction of  $\text{NO}_3^-$  reduces rapidly to zero. As the concentration of  $\text{NO}_3^-$  decreases, the concentration of  $\text{NO}_2^-$  builds which influences the kinetics of the three  $\text{NO}_2^-$  reduction

reactions. Later in the model predictions, the current efficiencies of the  $\text{NO}_2^-$  reduction reactions fall due to low concentrations. This coincides with an increase in the rate of water reduction. The effect of the increase in current density from 0.35 to 0.45  $\text{A}/\text{cm}^2$  shows an increase in the kinetic rate of the cathodic reactions.

Table 1: Physical, Mass Transfer, and Kinetic Properties (Temperature = 298.15 K)

Catholyte Volume:	700 ml
Anolyte Volume:	7000 ml
Electrode Gap:	0.6 cm
Separator Thickness:	0.05 cm
MacMullin Number ( $N_M$ ):	5.0
Volumetric Flowrate:	10.5 $\text{cm}^3/\text{sec}$
Kinematic Viscosity ( $\nu$ ):	1 cS
Solution Density ( $\rho$ ):	1 $\text{gm}/\text{cm}^3$
Initial $\text{NO}_3^-$ Concentration:	1.95 $\times 10^{-3}$ moles/ $\text{cm}^3$
Initial $\text{NO}_2^-$ Concentration:	0.60 $\times 10^{-3}$ moles/ $\text{cm}^3$
Initial $\text{OH}^-$ Concentration:	1.33 $\times 10^{-3}$ moles/ $\text{cm}^3$
Transfer Coefficient ( $\alpha$ ):	0.5 all reactions
Exchange Current Densities-	
reaction 4:	1.6 $\times 10^{-10}$ $\text{A}/\text{cm}^2$
reaction 5:	2.0 $\times 10^{-11}$ $\text{A}/\text{cm}^2$
reaction 6:	6.6 $\times 10^{-15}$ $\text{A}/\text{cm}^2$
reaction 7:	3.1 $\times 10^{-13}$ $\text{A}/\text{cm}^2$
reaction 8:	3.0 $\times 10^{-6}$ $\text{A}/\text{cm}^2$
anodic reaction:	1.9 $\times 10^{-11}$ $\text{A}/\text{cm}^2$
Electrons Transferred per Reaction-	
reaction 4:	1
reaction 5:	1
reaction 6:	1
reaction 7:	1
reaction 8:	1
anodic reaction:	4
Diffusion Coefficients-	
$\text{NO}_3^-$ species	1.902 $\times 10^{-5}$ $\text{cm}^2/\text{sec}$
$\text{NO}_2^-$ species	1.902 $\times 10^{-5}$ $\text{cm}^2/\text{sec}$
$\text{OH}^-$ species	5.260 $\times 10^{-5}$ $\text{cm}^2/\text{sec}$

Figure 5 shows the how the concentrations of  $\text{NO}_3^-$ ,  $\text{NO}_2^-$ , and  $\text{OH}^-$  in the catholyte change during the course of the experiment at current densities of 0.35 and 0.45  $\text{A}/\text{cm}^2$ . The concentration of  $\text{NO}_3^-$  decreases through the entire experiment while the concentration

of  $\text{NO}_2^-$  first increases, due to the rapid rate of  $\text{NO}_3^-$  reduction, then decreases. The concentration of  $\text{OH}^-$  increases to a steady value as the concentration of  $\text{NO}_3^-$  and  $\text{NO}_2^-$  fall. The final concentration of the  $\text{OH}^-$  will depend on the rate of mass transport of  $\text{H}_2\text{O}$  across the separator which is not calculated in this model.

Figures 6 and 7 show how the total cell potential and its components change during the experiment. In figure 6 the reference potential for the reduction of water, the anodic reference potential, and the anodic potential remain constant through the entire experiment. The cathodic potential decreases due to the kinetics of the cathodic reactions and the resistance losses increase due to the increase in the temperature of the cell. The total cell potential decreases to a steady value then increases slightly at the end of the experiment. This increase in the cell potential coincides with the onset of the water reduction reaction. This effect is more pronounced at lower current densities as shown in figure 7.

Figure 8 shows how the temperature of the cell is influenced by current density. At current densities of 0.35, 0.45, and 0.55  $\text{A}/\text{cm}^2$  a strong dependency of the temperature on the current density is apparent. The final temperature depends on the value of the heat transfer coefficient,  $U$ , which was assumed to be zero for this figure.

Figures 9 and 10 compare the model predictions with the experimental data taken in the apparatus shown in figure 1 with the current density of 0.5  $\text{A}/\text{cm}^2$ . Physical and Kinetic parameters shown in Table 1 were used. Comparison is quite good especially for the nitrate and nitrite species. It is interesting to note that the cell voltage drop for Celgard was higher than that for Nafion.

### Conclusions

A boundary layer model has been presented for the electrochemical reduction of nitrate and nitrite species in a parallel plate reactor. The model neglects migration but includes the dependency of simultaneous reactions on the surface concentration. The model agrees favorably with experimental data.

### Acknowledgement

This work was supported under Task No. 112 Contract No. AA00900T by Westinghouse/Savannah River Company. One of the authors (DAW) was a recipient of a DOE/EPSCOR Fellowship. The authors gratefully acknowledge this support.

### References

- [1] D.T. Hobbs and M.A. Ebra, in "Electrochemical Processing of Alkaline Nitrate and Nitrite Solutions", R.E. White, R.F. Savinell, and A. Schneider, Editors, AIChE Symposium Series, New York, NY (1987)
- [2] D. Genders, N. Weinberg, and D. Hartsough, in "Electrochemical Processing of Nitrate Waste Solutions," The Electrosynthesis Co. Inc., East Amherst, NY (1992)

- [3] D.H. Coleman, M.S. Thesis, Department of Chemical Engineering, Texas A&M University, College Station, TX (1993)
- [4] J.W. Van Zee and R.E. White, J. Electrochem. Soc., **133**, 508, (1986)
- [5] A.J. Bard and L.R. Faulkner, "Electrochemical Methods," page 109, John Wiley & Sons, New York, NY (1980)
- [6] J.S. Newman, "Electrochemical Systems," 2nd ed., page 31, Prentice Hall, Englewood Cliffs, NJ (1991)

//

Figure 1: Schematic Diagram

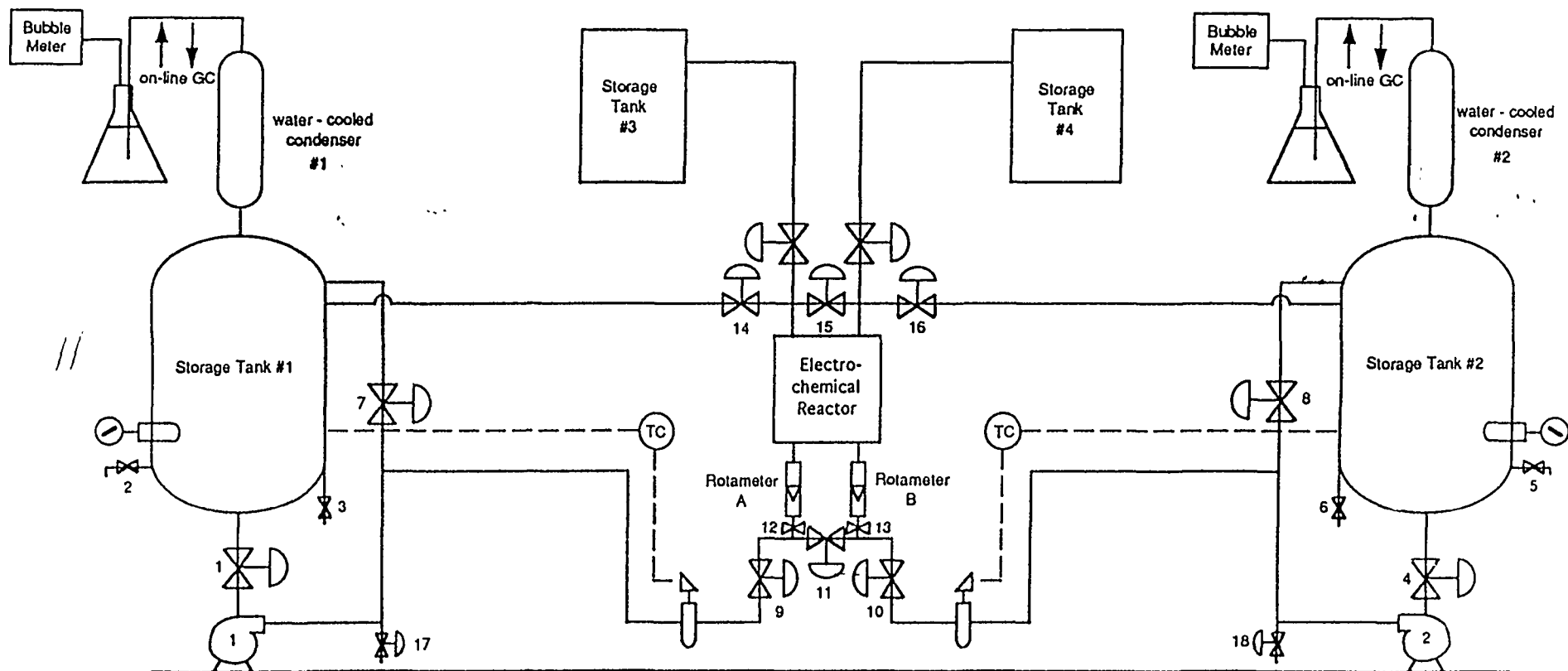


# Figure 2: MP Electrochemical Cell

Cross-Sectional Side View

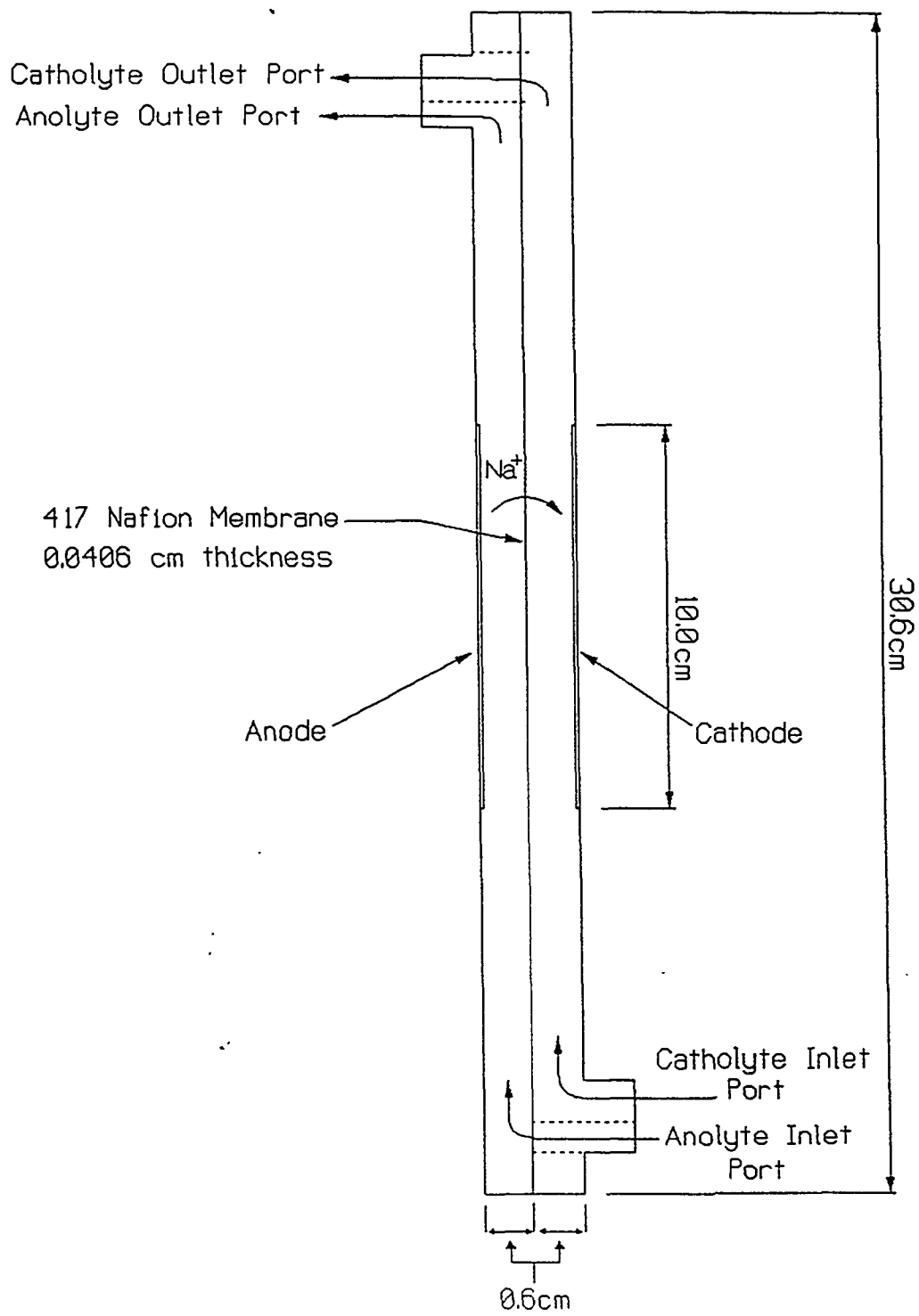


Figure 3: Electrolysis Current Efficiencies of NO<sub>3</sub>/NO<sub>2</sub> Reduction Process,  $i = 0.35 \text{ A/cm}^2$

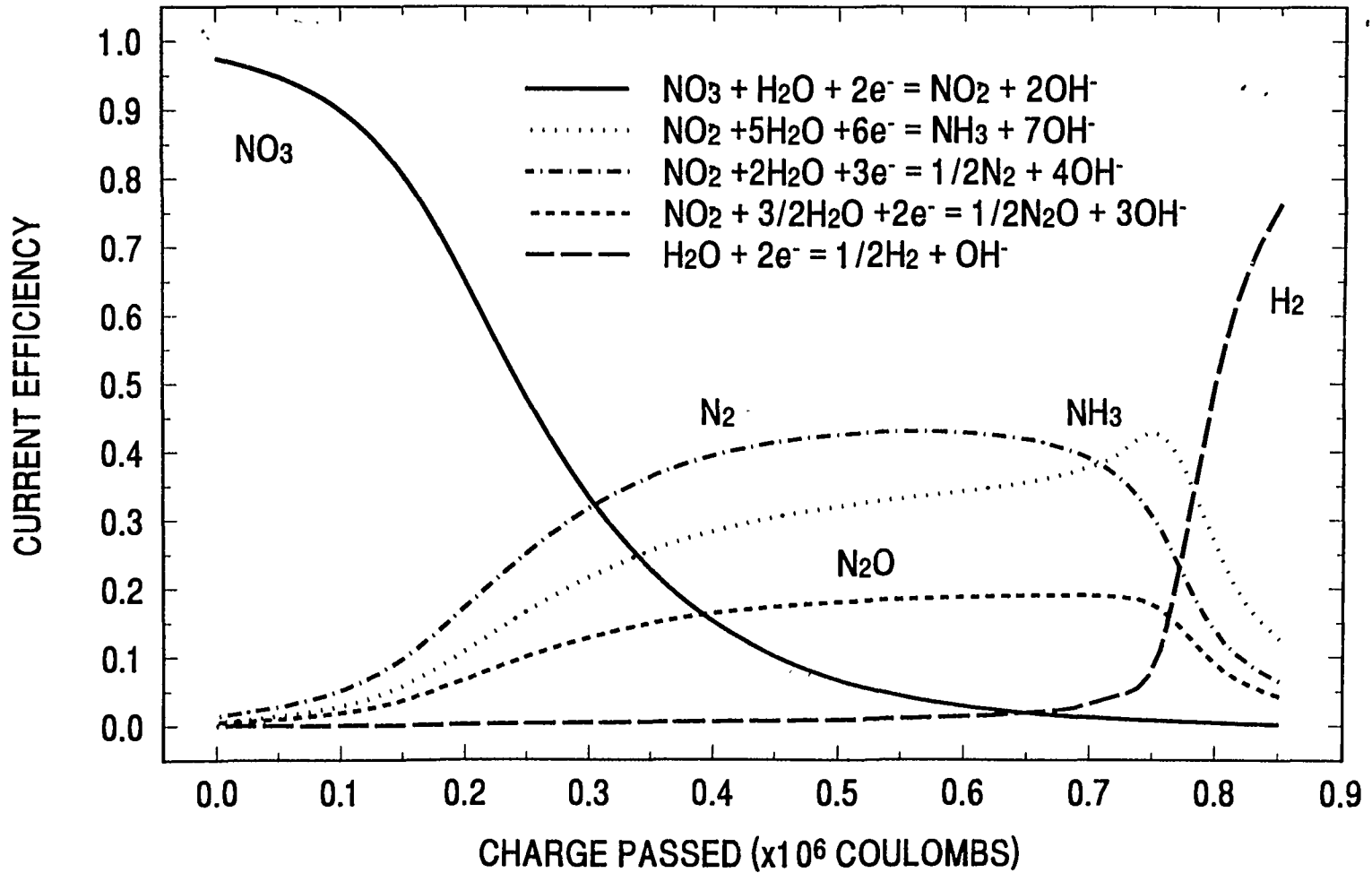


Figure 4: Electrolysis Current Efficiencies of NO<sub>3</sub>/NO<sub>2</sub> Reduction Process,  $i = 0.45 \text{ A/cm}^2$

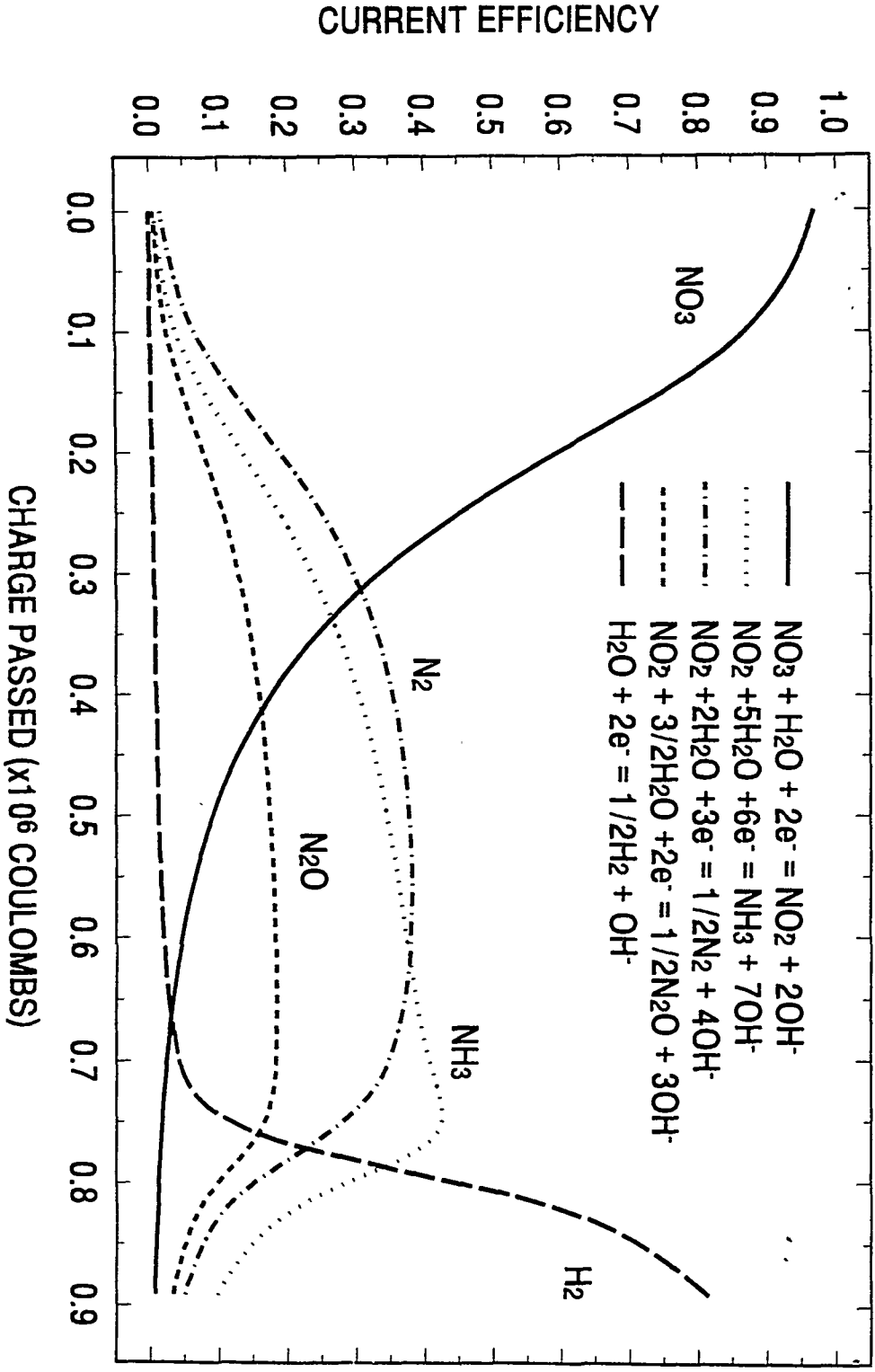




Figure 5: Catholyte Compositions of Major Components  
at  $i = 0.35 \text{ A/cm}^2$  and  $i = 0.45 \text{ A/cm}^2$

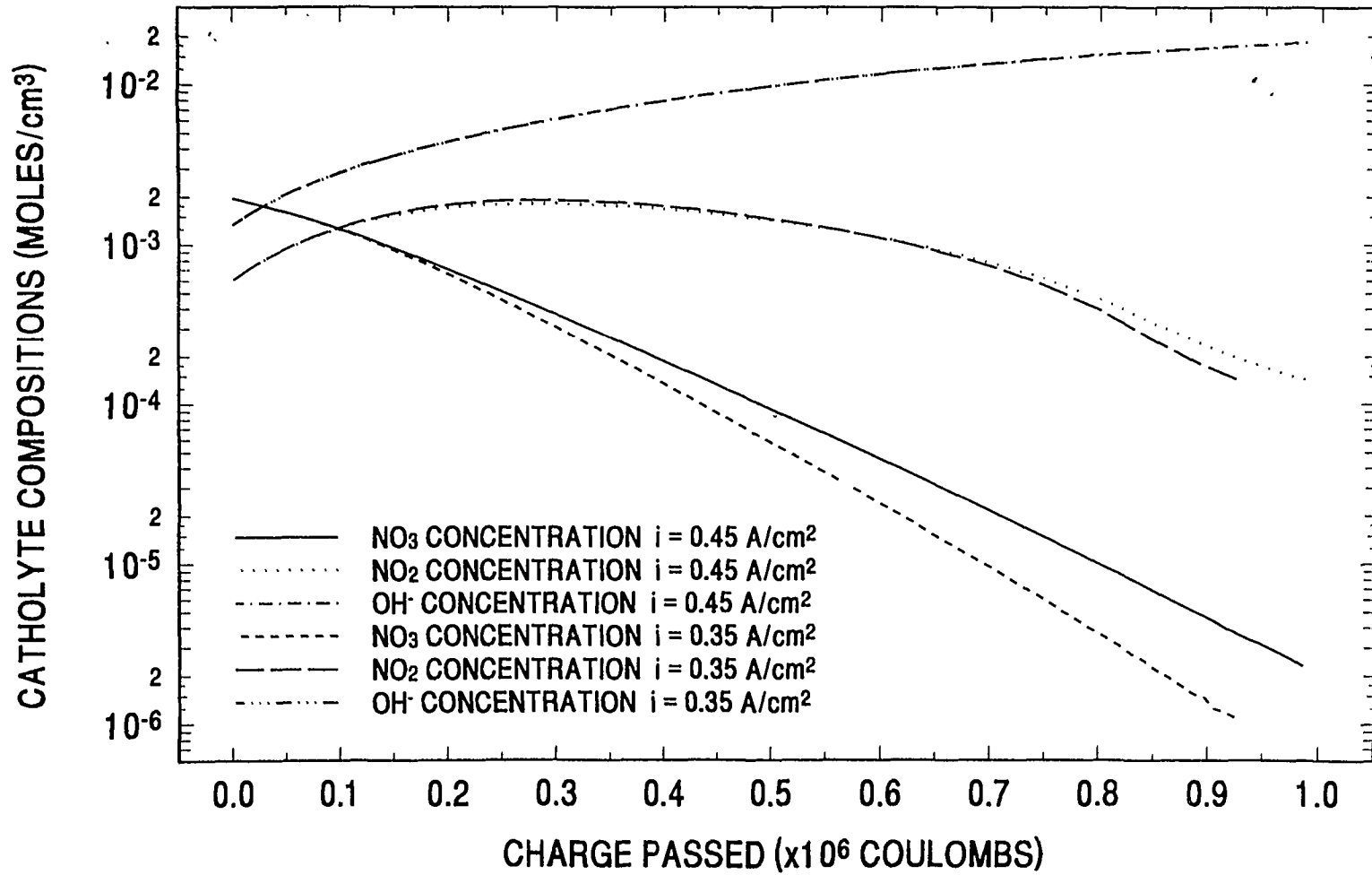


Figure 6: Components of the Cell Potential  
as a Function of Charge Passed

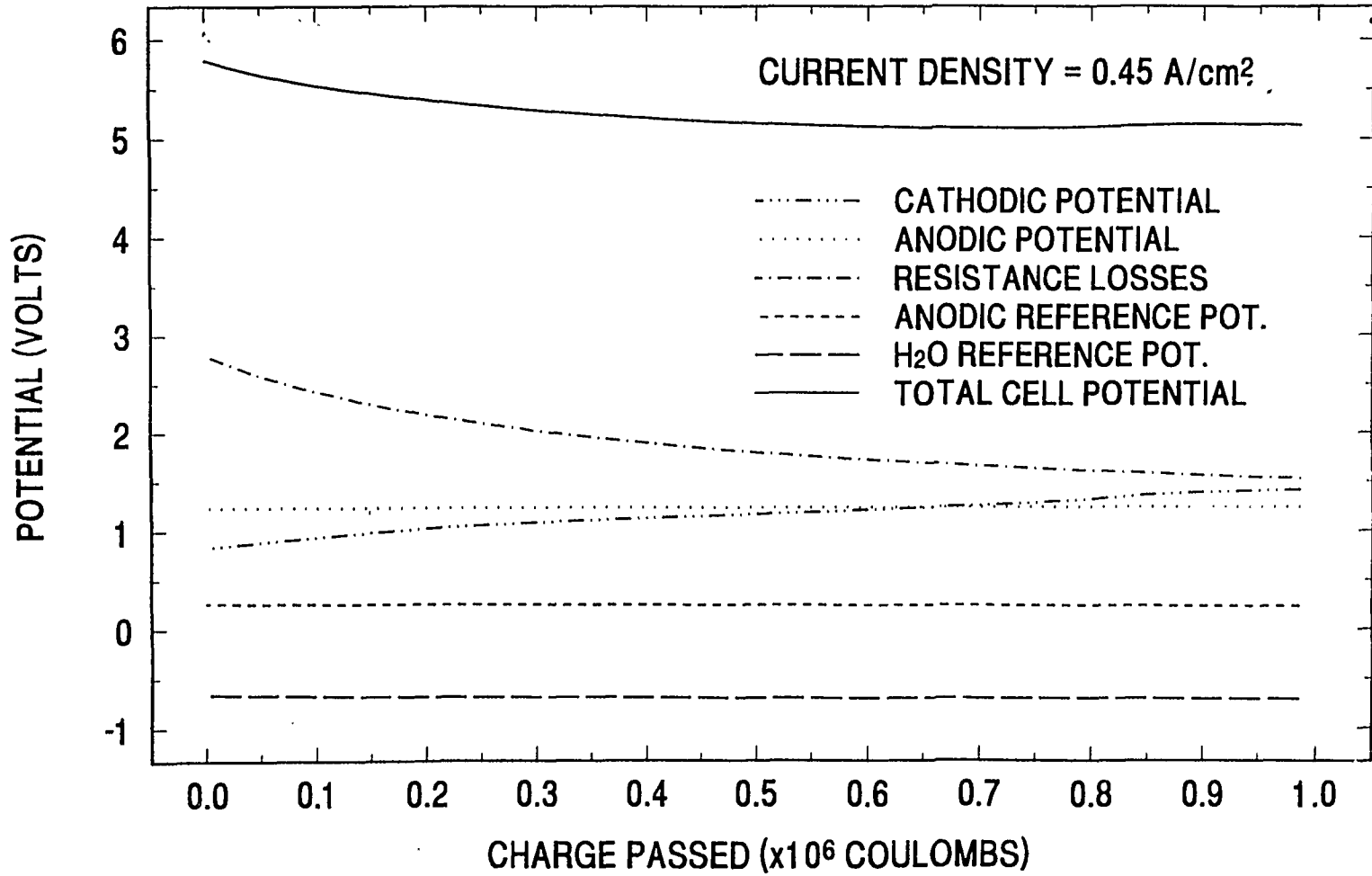
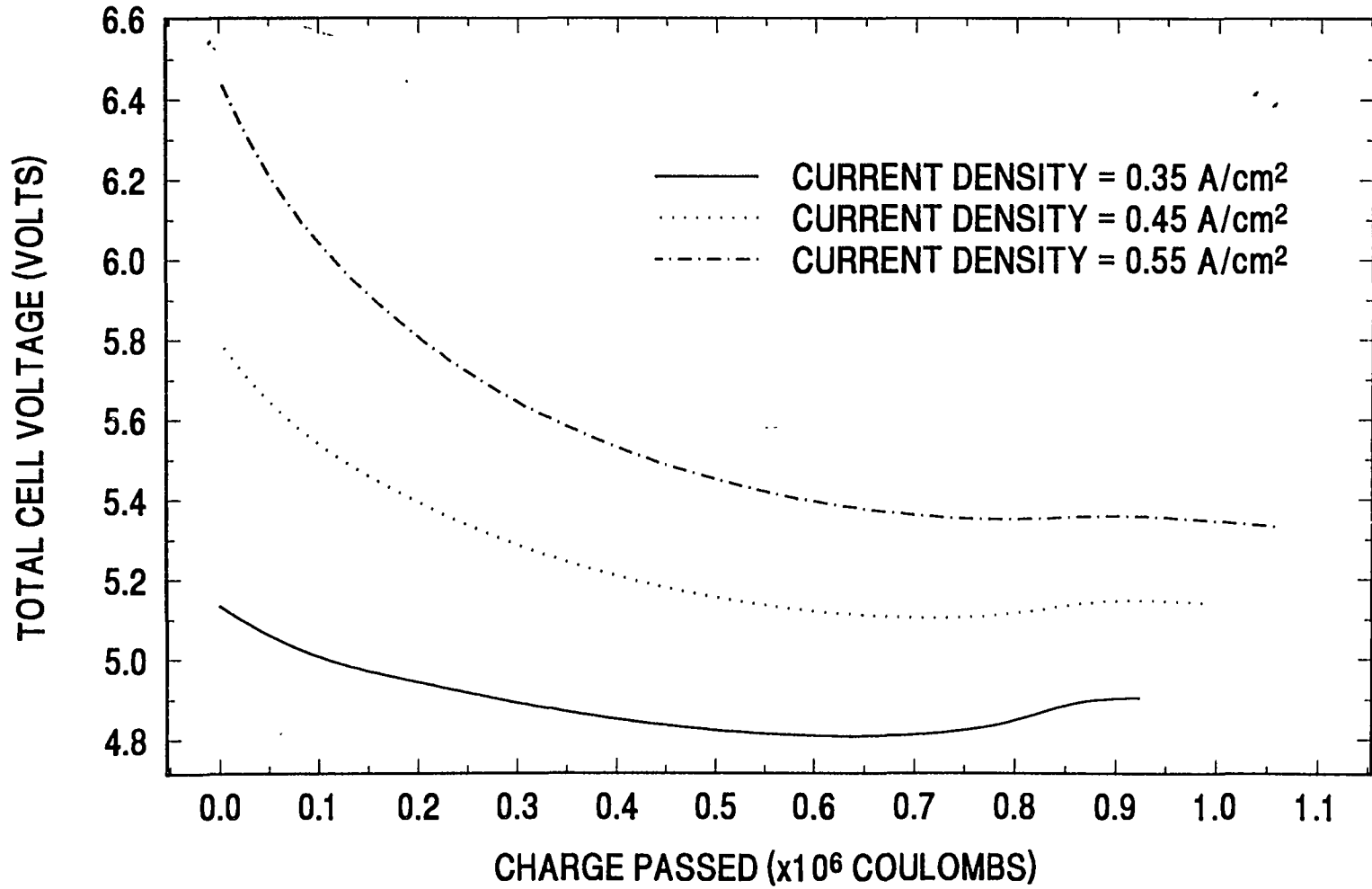


Figure 7: Effect of Current Density on Total Cell Voltage on Total Cell Voltage



11

Figure 8: Effect of Current Density  
on Cell Temperature

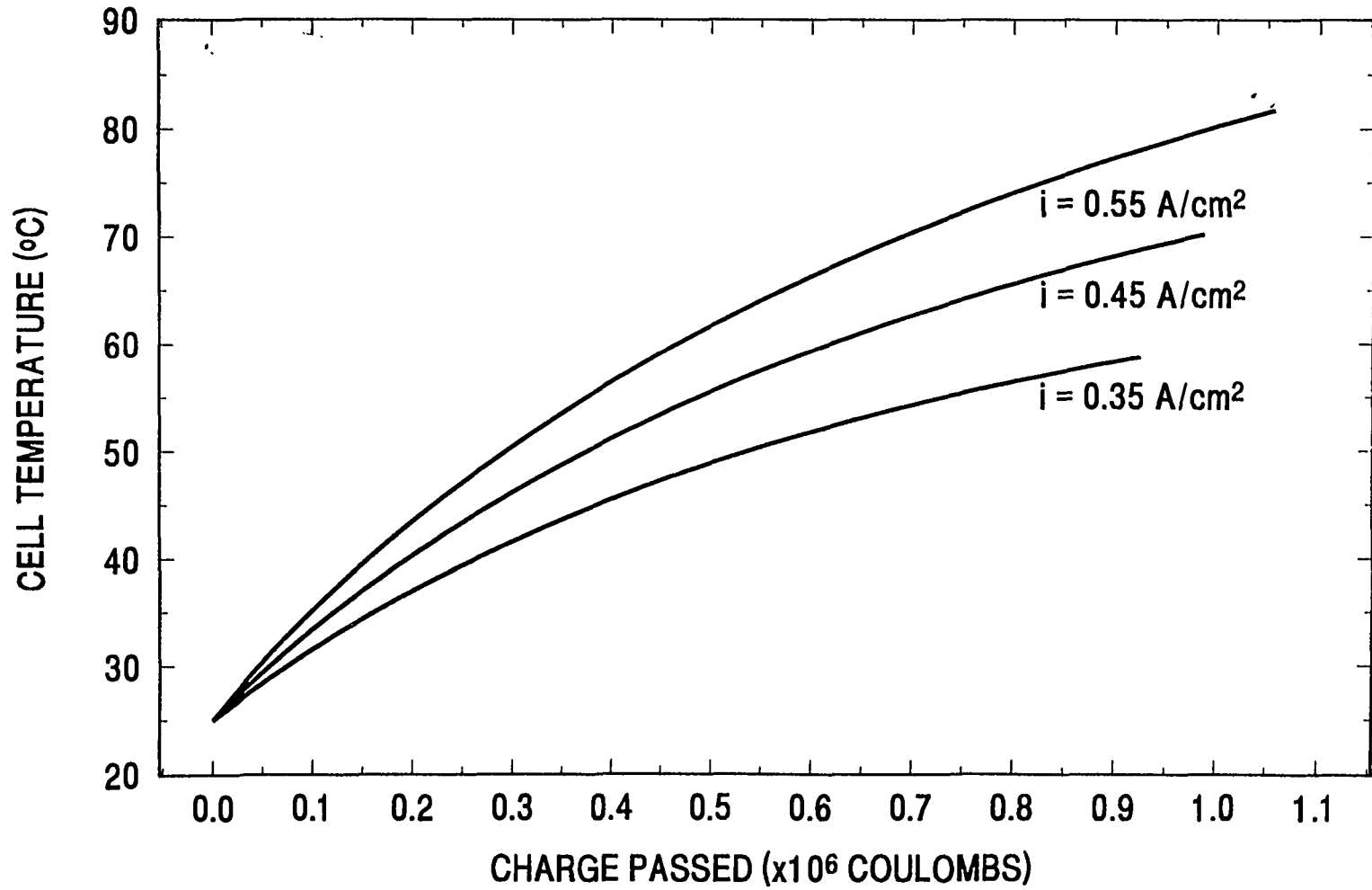


Figure 9: Compositions of Ionic Species in Run-3  
MP Cell, Pb/SS electrodes, Nafion 350

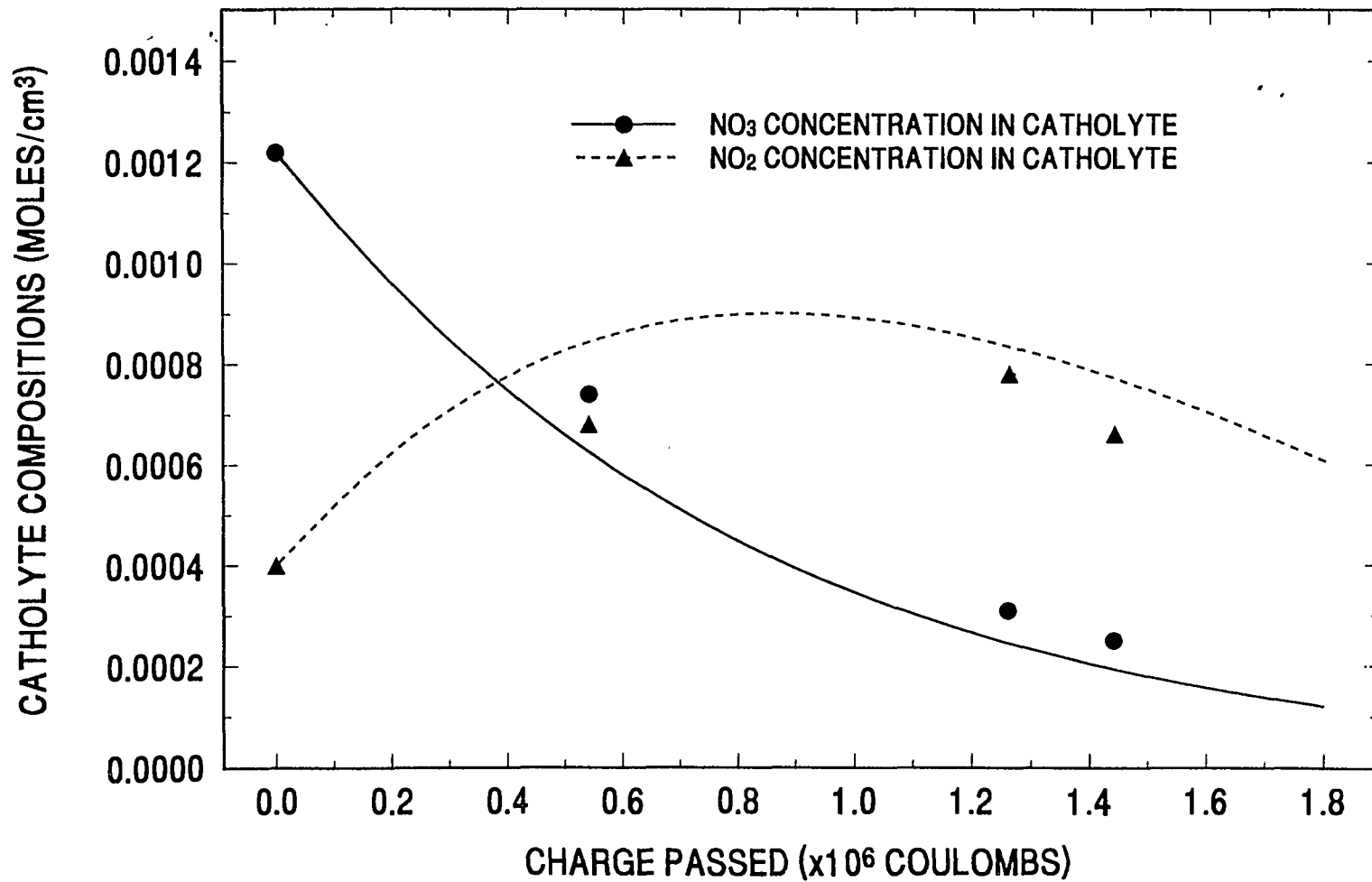


Figure 10: Model Predictions of Total Cell Voltage  
Versus Total Cell Voltage in Run-1 and 3  
MP Cell,Pb/SS electrodes,Nafion 350 and Celgard 3400

